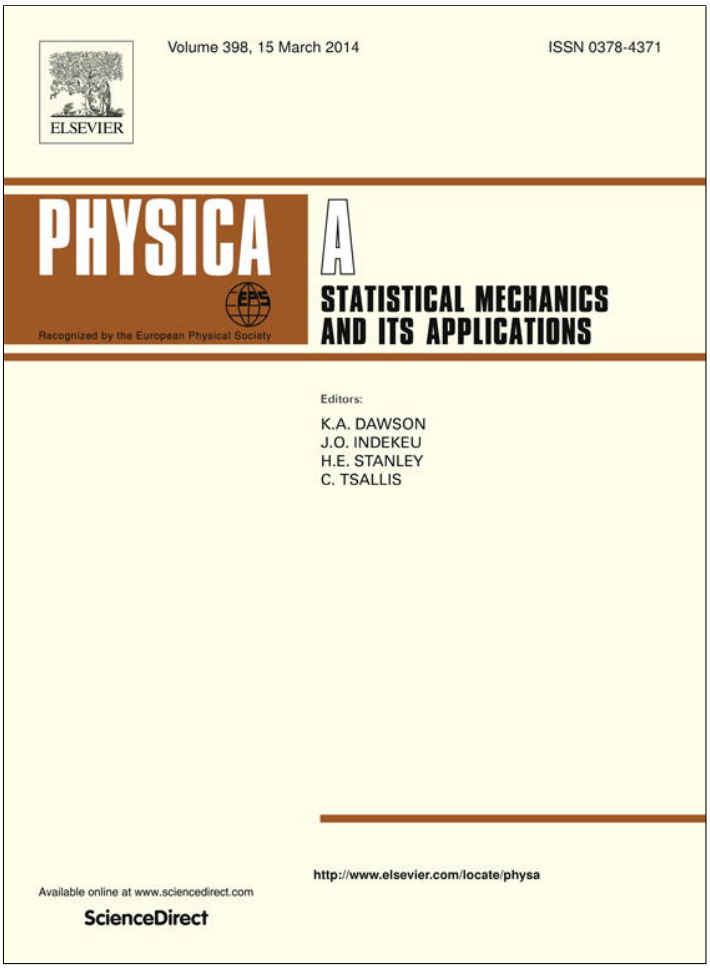

Physica A 398 (2014) 234–242

Contents lists available at ScienceDirect

Physica A

journal homepage: www.elsevier.com/locate/physa

Bond dimer percolation on square lattices

W. Lebrecht [a], J.F. Valdés [a], E.E. Vogel [a,*], F. Nieto [b], A.J. Ramirez-Pastor [b]

[a] Departamento de Física, Universidad de La Frontera, Casilla 54-D, Temuco, Chile

[b] Departamento de Física, Instituto de Física Aplicada, Universidad Nacional de San Luis-CONICET, Chacabuco 917, D5700BWS San Luis, Argentina

HIGHLIGHTS

- First analytic attempt for bond dimer percolation by means of analytic methods.
- Extrapolations towards the thermodynamic limit agree well with numeric results.
- Percolation thresholds are reported; they are lower than for bond monomers.
- Jamming coverage is obtained and discussed.
- Critical exponents are obtained and scaled; they are close to expected values.

ARTICLE INFO

Article history:
Received 3 September 2013
Received in revised form 16 December 2013
Available online 27 December 2013

Keywords:
Percolation
Bond dimer
Critical exponents
Scaling techniques

ABSTRACT

Percolation due to the simultaneous occupation of two neighboring bond sites, namely a bond dimer, is considered here by means of the renormalization cell technique providing an analytic way to obtain results such as percolation threshold, jamming coverage and critical exponents. This is complementary to previous numerical studies and extends the validation of the renormalization cell technique. Four different bond dimer depositions are considered: nematic, straight, angular and tortuous; results for each of them are given and analyzed separately. Size of the cells is varied. These results are combined with means of finite size scaling to obtain tendencies towards the thermodynamic limit. It is observed that the percolation threshold is reached at lower concentrations than for monomeric bond percolation establishing a trend for correlated bond percolation similar to the one already established for site dimer percolation. Two different techniques are used to obtain the percolation threshold getting results that are in good agreement with numerical simulations; similarly acceptable results for jamming coverage are obtained. Values for critical exponents are also in good agreement with those reported by means of numerical techniques.

1. Introduction

Most of the efforts done on bond dimer percolation have been based on computer simulations [1–3]. The main aim of the present paper is to provide an analytic approximation based on exact results for small cells that can be extrapolated to larger sizes. The successful comparison with the previously mentioned numerical results will provide a basis for the estimation of tendencies towards the thermodynamic limit.

This kind of percolation belongs to the class of percolation problems where the deposited object occupies several contiguous lattice positions (bonds in the present case) in what is called percolation by extended objects. In this case, the statistical problem becomes exceedingly difficult and a few studies have been devoted to understanding the percolation or deposition of elements occupying more than one place (site or bond) [4–14].

* Corresponding author. Tel.: +56 45 2325316; fax: +56 45 2325323.
E-mail address: eugenio.vogel@ufrontera.cl (E.E. Vogel).

0378-4371/$ – see front matter
http://dx.doi.org/10.1016/j.physa.2013.12.038

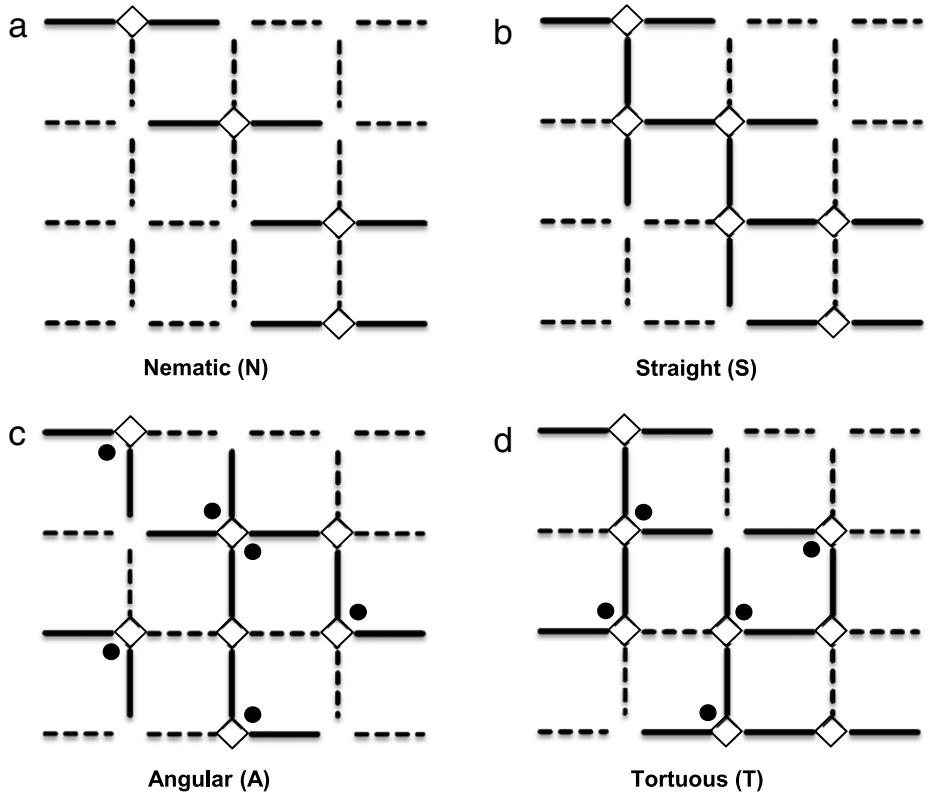

Fig. 1. Bond dimers depositions on a square lattice. (a) Nematic (N) only horizontal; (b) Straight (S) both horizontal and vertical with the possibility of crossing; (c) Angular (A) where the 90° angle is marked by a black circle; (d) Tortuous (T), which is a combination of all previous possibilities. Dashed and solid lines represent empty and occupied bond positions respectively.

Although a real case for a bond dimer is harder to realize than for a site dimer (diatomic molecule) its inclusion in the general study of percolating cases is of importance. On the other hand, a bond dimer is similar to a site trimer and establishes the onset of long percolating objects where the difference of bond or site percolation tends to dilute as the size of the object increases. This is on the line of studies including anisotropic percolation where the percolating object is long enough as to go over several lattice sites or bonds [15–17].

A bond dimer is defined as two nearest-neighbor bonds connected to a common site. We consider the case in which such dimer is rigid and remains as such after the deposition (it does not dilute) and the deposition is irreversible (it does not migrate through the lattice). No bond overlaps are allowed. As such, this is a case of local correlated percolation.

We will assume here a square lattice where we study percolation along the left–right direction which we call *horizontal* from now on (then *vertical* is the transversal direction). A portion of such lattice will be called a cell, which can be characterized by its frame and by its size. The frame is given by the vertical and horizontal edges, denoted by $q \times \ell$; The size is the number of constituent bond positions which for square cells corresponds to $\Gamma = q\ell + (q-1)(\ell-1)$, where q (ℓ) is the number of bond positions along the vertical (horizontal) direction.

We present below a basic analytic approach to obtain estimations for percolation threshold and critical exponents for the case of bond dimers; these results are then compared with computer simulations and results for similar systems available in the literature. Jamming coverage (saturation of dimer deposition leaving monomeric places unoccupied) will also be considered in the analysis below.

We follow here the approach of a recent paper dealing with dimer site percolation [18] for purposes of comparison. However, bond dimer percolation is different from dimer site percolation, so algorithms and simulations are also different from previous case. The most evident new feature is that here the two elements can have not only a linear ordering with two possible orientations similar to the site case, but the constituent bonds can also form a 90° angle with 4 different orientations. Thus the total number of possible occupation possibilities is 6.

Fig. 1 illustrates the different cases that could be present for bond dimer percolation on a square lattice. We have picked the particular case of a square cell of frames $q \times \ell = 4 \times 4$ where we consider different deposition possibilities. Fig. 1(a) shows dimer deposition with just left–right orientation: this percolation case will be called nematic (N). Then, Fig. 1(b) shows the case in which dimers can have both possible orientations in what will be called straight (S) dimers; in this case crossing of perpendicular dimers sharing a site is allowed. Fig. 1(c) presents the case in which the bonds forming the dimer span a 90° angle, which is depicted by a dot; this case will be called angular percolation (A); in this case two angular dimers can share a site. Fig. 1(d) presents a mixture of all previous depositions in what is called tortuous percolation (T); we shall assume equal probability for each of these six possibilities in the T case, leaving out of the analysis any kind of anisotropy in the lattice.

Each kind of deposition corresponds to a different possible real situation, so one of them could better represent a particular system. From this point of view we will consider them separately not attempting any average representation for them. Certainly the most especial case is the N deposition which will be left out of consideration in some particular cases below.

Depositions take place sequentially over random positions where both places to be occupied by the bond dimer must be empty. At the beginning dimers are isolated but at a certain point clusters or islands arise. Eventually one of these clusters grows large enough as to span the cell from left to right reaching percolation. The concentration of occupied positions at which this phenomenon is achieved is called percolation threshold and it is one of the goals of the present paper.

2. Results and discussion

Let p be the probability that a monomeric (M) bond position is occupied, then $1-p$ is the probability that such position is empty. Then the monomeric bond percolation function that gives the probability that a cell will percolate can be written in the following general form:

$$f_{\ell,\Gamma}(p) = \sum_{j=\ell}^{\Gamma} C^{j}_{\ell,\Gamma} p^{j} (1-p)^{\Gamma-j}, \tag{1}$$

where ℓ represents the number of horizontal bonds in the cell, and j is the number of bonds in the percolating cluster; it follows that $\ell \leq j \leq \Gamma$. The coefficients $C^{j}_{\ell,\Gamma}$ correspond to the number of possible configurations leading to monomeric percolation for a cell of horizontal dimension ℓ and total size Γ. The simple example for $C^{3}_{2,5} = 8$ as it can be appreciated from Fig. 19 of Ref. [19].

In the problem discussed here numbers are larger, for instance $C^{15}_{4,25} = 2.715.264$, is the number of different monomer bond configurations for a cell with horizontal length 4, where the total number of bond positions (size) is 25, and the particular case of percolating clusters of 15 elements ($j = 15$) is considered. We obtained this and all the other numbers reported below by means of a computational algorithm that generates all possible bond configurations for each cell.

It turns out that the percolation function for the case of monomer bond occupation on a square cell is a sigmoid with a fix point at $p_{ren} = 0.5$ which represents the percolation threshold obtained by renormalization (*ren*) methods. Namely, we need to solve the equation $f_{\ell,\Gamma}(p_{ren}) = p_{ren}$. Alternatively, the percolation threshold can be approximately obtained by finding the inflection (*inf*) point of the curve p_{inf}, namely, upon solving $f''_{\ell,\Gamma}(p_{inf}) = 0$.

This same technique can be employed for the cases of dimer percolation given in Fig. 1, provided the following adjustments are observed [18]:

(1) A dimer occupies simultaneously two empty nearest-neighbor positions compatible with its shape; the occupation probability d is the one of two monomer positions, namely, $d = p^2$. The corresponding probability for the same set of the same two positions to be empty is $(1-d)$. This procedure links these two positions, which is a characteristic of correlated percolation.

(2) The occupation process is carried out by stages of one dimer at a time up to saturation.

(3) Percolation is then studied according to the usually established rules independent of the kind of object that was deposited on the lattice.

(4) Since occupation is at random it is possible that some single positions remain empty and cannot be occupied by dimers. On one hand, this will lower the percolation threshold. On the other hand, the occupation of the cell will not always saturate reaching a maximum filling in what is known as *jamming coverage*. This phenomenon will require a renormalization of the percolation function taking into account those configurations that are really reachable. This is done in the following way:

$$f_{L,D}(d) = \frac{n_{L,D}(d)}{m_{L,D}(d)} = \frac{\sum_{j=L}^{D} G^{j}_{L,D} d^{j} (1-d)^{D-j}}{\sum_{j=0}^{D} H^{j}_{L,D} d^{j} (1-d)^{D-j}} \tag{2}$$

where L represents the number of percolating objects along the horizontal direction. Then j varies in the interval $L \leq j \leq D$, D being the maximum number of dimers for the particular cell. The coefficients $G^{j}_{L,D}$ correspond to the number of possible configurations with a given percolation length j. Coefficients $H^{j}_{L,D}$ represent the total number of configurations for a given j, regardless whether they percolate or not. Then it is obvious that $G^{j}_{L,D} \leq H^{j}_{L,D}$.

Table 1 yields the corresponding values for previous quantities applied to the four dimer cases shown in Fig. 1. This is done for the same particular choice of $j = 15$ used in the case of monomeric occupation so a direct comparison is possible. Size in each case is arbitrary and appropriate for the illustration purpose of this table. We begin by discussing the N case in detail; other cases just follow this same approach. In the case of N occupation we illustrate the system by means of an 8×6 cell, leading to a size $\Gamma = 83$ bond places, with $L = 3$ dimers directly percolating from left to right.

Table 1
Number of percolating trajectories $\Gamma^{15}_{L,D}$ and total trajectories $H^{15}_{L,D}$ associated to the four dimers N, S, A, and T for different sizes.

Cell frame	Dimer	Γ	L	D	$G^{15}_{L,D}$	$H^{15}_{L,D}$
8×6	N	83	3	24	58,578,352	69,775,792
6×6	S	61	3	30	18,011,893,092	25,977,230,320
5×5	A	41	5	16	143,207,960	146,236,904
5×4	T	32	2	16	368,584	368,584

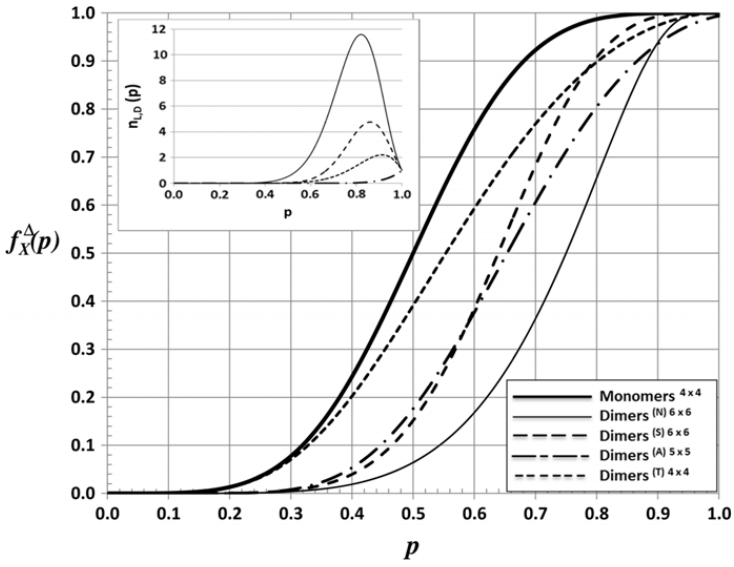

Fig. 2. Bond percolation function associated to monomers (M) and dimers (N, S, A, and T). The jamming coverage values can be obtained by the maxima of the functions given in the inset, obtained through the numerator of Eq. (2).

The maximum number of nematic dimers occupying this cell is given by $D = q[\ell/2]$, where [] represents the integer part of the result obtained from using this expression, which turns out to be 24 for this example. The number of percolating configurations with $j = 15$ is given in the next column under $G^{15}_{L,D}$, which in this case is smaller than the total number of configurations $H^{15}_{L,D}$. An analogous interpretation for the columns of this table can be applied to the other occupation cases. The corresponding expressions for column D are as it follows: $D = q\ell/2 + (q-1)[(\ell-1)/2]$ for S; $D = (q-1)(\ell-1)$ for A; $D = [(q\ell + (q-1)(\ell-1))/2] = [\Gamma/2]$ for T.

Values in this table may appear a bit surprising at a first look. However, there is always a rationale behind these numbers. Thus, for instance, the cell 6×6 used for the S case yields larger $G^{15}_{L,D}$ and $H^{15}_{L,D}$ coefficients than the larger cell 8×6 used for the N case due to the fewer possible rearrangements originating partly in the lack of vertical connectors for the latter. Another curiosity in this table is that the cells picked for the A and T cases both have the same D value (16) but their results for $G^{15}_{L,D}$ and $H^{15}_{L,D}$ coefficients are enormously different. The reason for this can be found in the more possibilities of accommodation for the A case which leaves more empty places for dimer occupation than the equivalent example for the T case which saturates, so the all of them percolate making $G^{15}_{L,D} = H^{15}_{L,D}$. This last result is general for the case of large enough occupation ratios and it is also true for the case of site dimer occupation as shown in Fig. 2 of a recent paper [18]. Several other special cases could be discussed from Table 1 or a more general version of it, but we leave this discussion at this point.

Fig. 2 aims to illustrate the percolation analysis putting both monomeric and dimeric percolation in the same footing recalling that $d = p^2$. Then the percolation functions $f_X^{\Delta}(p)$, where Δ identifies the deposition ($\Delta = M, N, S, A, T$) and X absorbs both size indices (L, D or ℓ, Γ). Curves represent the bond percolation functions for several kinds of percolation on a square cell of size 4×4. As a reference we also include the case of bond monomers which is shown by a thick continuous line; this curve was obtained by solving the Eq. (1) above.

The analysis below is based on calculations for the following cells: (a) 4×6, 5×6, 6×6, 7×6 and 8×6 for N percolation; (b) 4×4, 5×4, 6×4 and 7×4 for S percolation; (c) 4×4, 4×5, 5×4, and 5×5 for A percolation; (d) 3×3, 4×3, 3×4, 4×4, 4×5 and 5×4 for T percolation. Occupancy considers all possibilities of orientations of the appropriate dimer according to each percolation case (N, S, A or T). In the asymmetric cases of same size for the T case an average value for the observables is considered [18].

Percolation functions for bond dimers included in Fig. 2 are obtained by solving Eq. (2) for square cells of sizes: 6×6 for N and S, 5×5 for A, and 4×4 for T. Fig. 2 represents the percolation functions for all the deposition cases presented in Fig. 1 plus the percolation function for monomeric bond occupation included here for comparison purposes; a particular size is chosen for each deposition. For $f_X^{\Delta}(p) = 0.5$ ($\Delta = M, N, S, A, T$) curves follow an order from left to right: M, T, S, A,

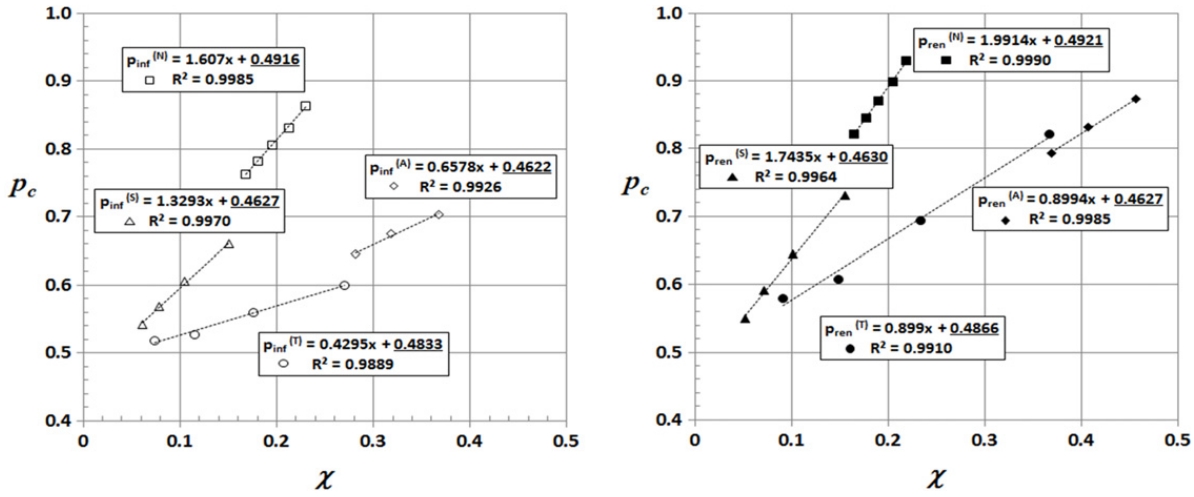

Fig. 3. Finite scaling plots to determine the bond dimer percolation according to depositions N, S, A, and T. Left-hand side: using the inflection point of the percolation function; Right-hand side: using renormalization techniques.

and N; eventually such an order is not the same in the thermodynamic limit. However, such an order is changed for larger values of p due to the nature of each of the percolation functions. Thus, S overcomes T just under $p = 0.80$. More striking is the case of the A function which goes under S at $p = 0.56$ and then goes under N at $p = 0.90$ reaching the end of the range without saturation.

We turn now our attention to the inset of Fig. 2 which considers the numerator of Eq. (2) which determines jamming coverage [18]. A maximum is observed for N, S, and T, which correspond to the jamming coverage of each case; this behavior is characteristic of correlated percolation. In the particular case of A dimers of the small size studied here, the numerator of Eq. (2) does not show a maximum. Of course here we leave out of any consideration the M case since for monomeric occupation there is no problem in saturating the lattice.

For the 6×6 cell used in the N case we observe that the numerator of Eq. (2) maximizes near $p = 0.8$ which corresponds to the jamming coverage in this particular case. Similarly, we find maxima for the 6×6 cell used in the S occupation and for the 4×4 cell used in the T deposition. For the 5×5 cell used in the A case no maximum was found, which was also the result for other cells with A occupancy. Upon taking into consideration the cells considered in the present study defined above we can obtain average jamming coverages for the different depositions: 0.8248 for N, 0.8178 for S and 0.8890 for T. Jamming coverage associated to the T case is greater than the other two, since the deposition for this system involves six possible orientations. Average values for jamming coverage associated to N and S cases are very similar between them. The overall average value given by these 15 cells is 0.8486. If the N case is excluded the resulting average considering both S and T depositions turns out to be 0.8605, which is very close to 0.863(2) obtained by means of numerical simulations [3].

The percolation threshold is then calculated by means of the two procedures p_{ren} and p_{inf} previously described. Results are illustrated in Fig. 3, for each kind of percolation: N, S, A and T. Scaling techniques will be used to obtain results valid for the thermodynamic limit.

Functions will be obtained in terms of the minimum percolation length which we called ℓ for monomers and L for dimers. It follows that $L = 2\ell$.

In this treatment we can consider second-order approximations for the percolation threshold which allows to write

$$p_{ren(inf)}(\ell) \sim p_c + \ell^{-1/\nu}(a + b\ell^{-1} + c\ell^{-2} + \cdots +), \tag{3}$$

where a, b, and c are adjustable parameters; ℓ represents the minimum percolation length in the left–right direction; ν is the usual critical exponent which we take here with its theoretical value 4/3. All critical exponents are discussed in a special section below.

Results are presented in Fig. 3 where the ordinate axis represents the percolation threshold given in terms of χ, which is a scaled variable that takes care of finite size corrections defined as:

$$\chi = \ell^{-1/\nu}(a + b\ell^{-1}). \tag{4}$$

In this way the percolation thresholds for the cases under study can be obtained. Thus, the percolation thresholds for the N case are 0.4921 and 0.4916 according to p_{ren} or p_{inf} respectively (we adopt this order in the remaining discussion); in both cases the regression coefficient is close to 1.0. It can be noticed that this result is very close to the one for bond monomers whose percolation threshold is 0.5. For the S case the percolation thresholds are 0.4630 and 0.4627 respectively; for the A case results are 0.4627 and 0.4622 respectively; for the T case we obtain 0.4866 and 0.4833 respectively. These results are in good agreement with those obtained by means of different numerical techniques [2,3]. It can be noticed that the percolation threshold is larger for N as compared to the other cases, a result which is similar to the one obtained for site dimer percolation [3]. However, N percolation is quite unique as it lacks vertical connectors so percolation can be established

in a direct way only. When considering the other 3 depositions the highest percolation threshold corresponds to the T case which shows 6 possible orientations.

The percolation threshold for the N case is higher than for the S case. Such behavior has been already observed numerically for site k-mers on a square lattice [10–13] and it is consistent with previous theoretical studies [15,16]. In addition it is also confirmed by experimental data about carbon nanotubes percolation in polymer composites, where a growth in the alignment of the nanotubes produces an increase in the percolation threshold [17].

The percolation thresholds for the S case reported above are in excellent agreement with numeric simulations where a value 0.464(2) is reported [3]. Such a value is lower than the one for the T case, a tendency which has been observed in the case site k-mers on a square lattice [2].

3. Critical exponents ν, β and γ

The criticality of a percolating system is associated to an order parameter. The way in which such an order parameter behaves near a critical point is represented by the exponent of a function. In its own turn this critical exponent characterizes the universality of the system according to the its dimensions. In what follows critical exponents ν, β and γ are studied considering corrections to the scaling laws as given by Reynolds et al. [20].

The critical exponent ν is associated to the order parameter ξ representing the correlation length, which diverges at the percolation threshold. Its formal definition is:

$$\xi \sim \mid p - p_c \mid^{-\nu} \quad p = p_c. \tag{5}$$

On the other hand, we can make use of a relationship involving ν which can be obtained by means of renormalization techniques:

$$\ln \ell = \nu \ln \lambda^*, \tag{6}$$

where λ^* represents the maximum value of the first derivative of the percolation function at $p = p_c$ in the limit of a cell of infinite dimensions.

For finite cells we can define $\frac{f_X^{\Delta}(p) - f_X^{\Delta}(p_c)}{(p - p_c)} = \lambda_X^{\Delta *}$, after a first-order approximation in the Taylor series for Eq. (1) at $p = p_c$. In this way $\lambda^{\Delta *}$ corresponds to the maximum value of the first derivative of the function $f_X^{\Delta}(p)$.

The higher the degree in the polynomial describing $f_X^{\Delta}(p)$ the better the approximation near the critical point leading to its divergence, namely, $\lambda^{\Delta *}$ tends to diverge at this point. However, we deal with finite size cells in whose case $\lambda^{\Delta *}$ maximizes at the critical point reaching a value that depends both on the cell size Γ and on the minimum percolation length ℓ. Such a maximum value will be denoted as

$$\lambda^* = W_X^{\Delta} \lambda_X^{\Delta *}, \tag{7}$$

where W_X^{Δ} is a multiplier which makes now $\lambda_X^{\Delta *}$ maximum at the critical point.

Combining Eqs. (9) and (10) we find:

$$\frac{1}{\nu} = \frac{\ln W_X^{\Delta}}{\ln \ell} + \frac{\ln \lambda_X^{\Delta *}}{\ln \ell}, \tag{8}$$

or equivalently

$$\frac{\ln \lambda_X^{\Delta *}}{\ln \ell} = \frac{1}{\nu_X^{\Delta}} = \frac{1}{\nu} - \frac{\ln W_X^{\Delta}}{\ln \ell}. \tag{9}$$

Exponent β is associated to order parameter P_∞ when the probability of occupation p is over the percolation threshold p_c. Analogously, exponent γ is associated to order parameter S_s, which characterizes the average size of clusters approaching p_c from lower values of p. The formal definitions of these two exponents are:

$$P_\infty \sim (p - p_c)^{\beta} \quad p > p_c \qquad S_s \sim \mid p - p_c \mid^{-\gamma} \quad p < p_c. \tag{10}$$

Eqs. (1) and (2) lead us to functions P_∞ and S_s, which can be studied for the appropriate interval, either $p > p_c$ or $p < p_c$. Then the critical exponents β and γ are determined from the slopes in the corresponding log–log plots for appropriate variables.

Fig. 4 represents the reciprocal value of the critical exponent ν for bond dimers in accordance to their orientation, S (empty triangles), A (empty diamonds) or T (empty circles). The analysis goes over symmetric cells $\ell \times \ell$ as well as over asymmetric cells in whose case the reported value corresponds to the arithmetic average between cells $\ell \times (\ell + 1)$ and $(\ell + 1) \times \ell$. We leave out of the critical exponent analysis the N case where the progression is directly along the percolation direction saturating quickly for the small size cells considered here. Additionally, frames with odd ℓ values along the horizontal direction are impossible in the N case.

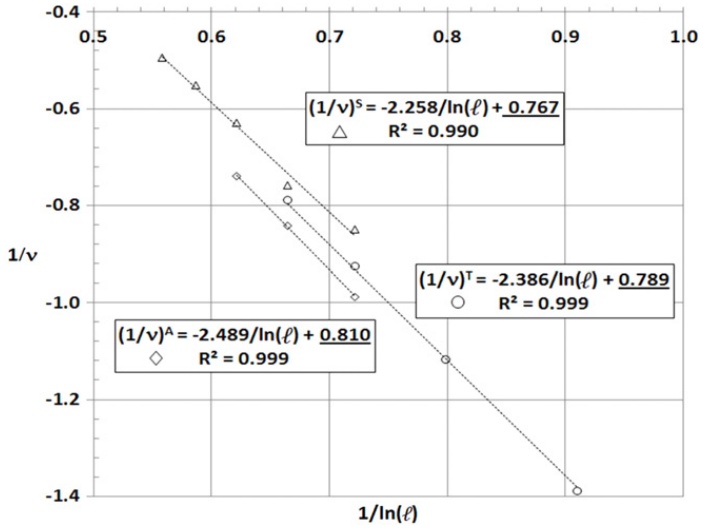

Fig. 4. Determination of critical exponent ν for bond dimers on the square lattice.

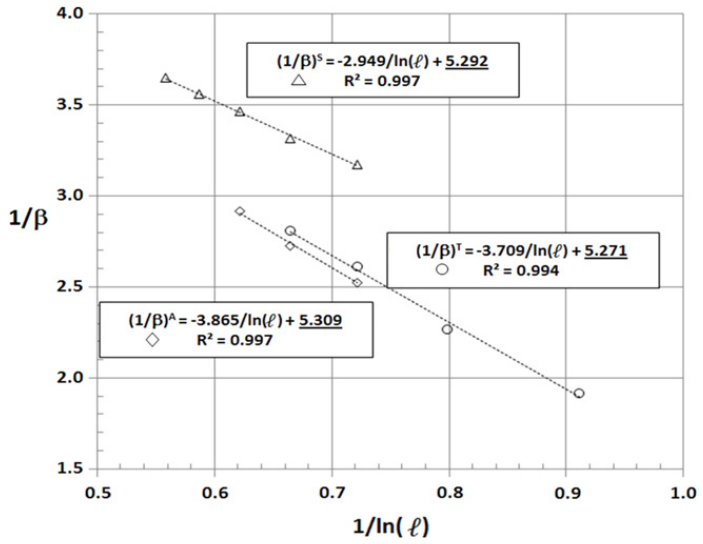

Fig. 5. Determination of critical exponent β for bond dimers on the square lattice.

The values for ν obtained from this analysis, namely, 1.304 for S, 1.235 for A, and 1.267 for T are very close to the ideal expected value for monomers which is 4/3 [19]. It can be noticed that in both cases the regression is quite good.

In Fig. 5 we report the reciprocal value for β in the case of bond dimers according to their orientation, S (empty triangles), A (empty diamonds) or T (empty circles). The procedure considers symmetric and antisymmetric cells as described for previous figure. By the same reasons given in previous analysis nematic percolation is left out. The values obtained for β are 0.189 for S, 0.188 for A, and 0.190 for T, both not to far from the ideal value for monomers which is 5/36 [19].

In Fig. 6 we report the reciprocal value of critical exponent γ in the case of bond dimers according to their deposition S (empty triangles), A (empty diamonds) or T (empty circles). Previous considerations on S, A, and T deposition and values for asymmetric cells also apply here. The values obtained for γ are 2.404 for S, 2.353 for A, and 2.370 for T. These values are close to the ideal value for monomers which is 43/18 [19].

As a way to condensate and compare these results with reports for other percolating object we construct Table 2. From this perspective several comments are possible.

Results for ν are very encouraging from two points of view: (1) they are close to the exact value for monomer percolation which is 4/3 [19] and (2) they are in general good agreement with previously published numeric results for percolation by site dimers [2,18].

In the case of β our values are larger than the ideal one for monomers (5/36); however, our three values are very consistent among themselves. This compares well with the disperse results reported for site dimer percolation [2,10,18].

Our γ values present a dispersion around the ideal value for ordinary percolation, namely, 43/18. Similarly, values for site dimer percolation reported in the literature present an even larger dispersion [2,10,18].

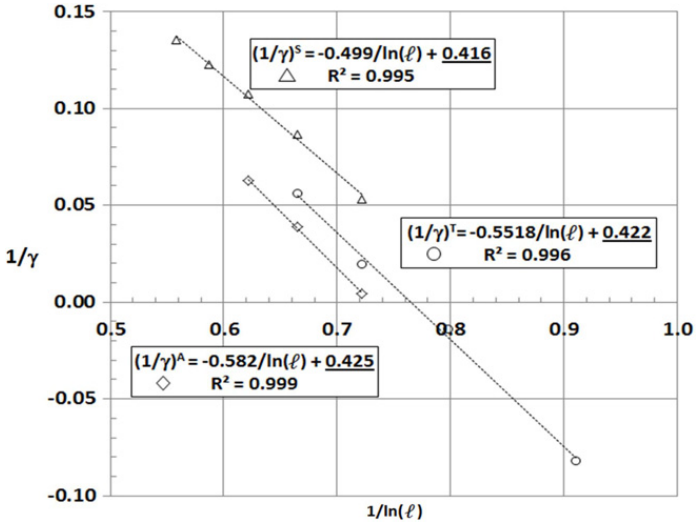

Fig. 6. Determination of critical exponent γ for bond dimers on the square lattice.

Table 2
Resume of values for critical exponents ν, β and γ for different percolating objects. As a general reference we include the theoretical values for bond monomers M; next three columns refer to bond dimers according to depositions S, A, T; we close with reported values for site dimer percolation for comparison purposes. References are listed following the general codes of the list at the end: asterisks identify results obtained in the present paper.

Crit. exponent	M Ref. [21]	S^*	A^*	T^*	Site dimers Refs.
ν	$\frac{4}{3} \approx 1.333$	1.304	1.235	1.267	1.368, 1.373 [2] 1.491 [14]
β	$\frac{5}{36} \approx 0.139$	0.189	0.188	0.190	0.121 [2] 0.179 [10] 0.194 [14]
γ	$\frac{43}{18} \approx 2.389$	2.404	2.353	2.370	2.452 [2] 2.375 [10] 2.394 [14]

4. Conclusions

The approach used in the present paper shows that it is possible to tackle k-mer percolation by means of renormalization methods. In particular finite size scaling using relatively small percolation cells yield linear regressions which are remarkably good.

The application of this technique to bond dimers allows us to discuss different types of percolation (Nematic N, Straight S, Angular A, and Tortuous T) under the same description allowing for comparison of their similarities and differences.

Dimer percolation in general is the simplest correlated percolation. In this way we can obtain some analytic description of the jamming phenomenon usually obtained by the numerical approach. The results reported here by evaluation of analytic expressions are in good agreement with values reported by means of numerical simulations.

The values obtained for percolation threshold for N, S, A, and T are consistent among themselves and comparison with numeric results whenever possible shows good agreement. Generally speaking the percolation threshold for bond dimer percolation obtained by two different methods (renormalization and inflection point) is lower than bond monomer percolation thus marking the expected tendency for bond k-mer percolation.

Actual values for percolation thresholds obtained by the two analytical methods used here differ little among the different deposition cases as shown in the discussion above following Fig. 3. It is found that the decrease of the percolation threshold (which is 0.5 for the M case) is the following N (0.4921 and 0.4916), T (0.4866 and 0.4833), S (0.4630 and 0.4627) and A (0.4627 and 0.4622), using the conventional order (p_{ren}, p_{inf}). It is remarkable that values are basically independent of the method used to obtain the percolation threshold for each case.

Jamming coverage is lower for S deposition (0.8178) since it is possible to accommodate independently linear bond dimers in any of the two directions. The jamming coverage increases just a bit (0.8248) when the vertical direction is not longer allowed. When only A deposition is considered the occupancy by one bond dimer immediately affects both horizontal and vertical progression not allowing saturation. Such a situation is relaxed when admixture with straight dimers is considered in the T case which shows the largest possible jamming coverage (0.8890).

Jamming coverage for the T deposition turns out to be the largest one (0.8890), reflecting its higher connection of both horizontal and vertical bonds. On the contrary S deposition presents the minimum jamming coverage due

Values obtained for critical exponents ν, β, and γ are in good correspondence with similar results for other types of percolation. There is a dispersion among the different types of deposition S, A, and T, which can be expected especially for the small size of the cells considered here. However, the linear regressions done using scaling techniques show high R values indicating that critical exponents within each deposition also have a meaning.

Previous results are very encouraging for the use of the renormalization cell technique for k-mer percolation with $k > 2$. As it follows from all previous results and analysis it is possible to obtain good values in real space for both percolation threshold and critical exponents. The method shown here is very promising for dealing with more complex percolating systems, heterogeneities and different kind of lattices.

Acknowledgments

Two of us (WL and JFV) acknowledge partial support from Dirección de Investigación de la Universidad de La Frontera (DIUFRO), Chile, under contract DI 13-0102. One of us (EEV) is grateful to Fondecyt (Chile) under contract 1100156, Millennium Scientific Initiative under contract P06-022-F for partial support, and Centro para la Nanociencia y Nanotecnologia (CEDENNA) financiamiento Basal project FB0807 (Chile). F.N. and A.J.R-P. thank support from Universidad Nacional de San Luis (Argentina) under project 322000, CONICET (Argentina) under project PIP 112-201101-00615 and the National Agency of Scientific and Technological Promotion (Argentina) under project PICT-2010-1466.

References

[1] V. Cornette, A.J. Ramirez-Pastor, F. Nieto, Physica A 327 (2003) 71.
[2] V. Cornette, A.J. Ramirez-Pastor, F. Nieto, Eur. Phys. J. B 36 (2003) 391.
[3] M. Dolz, F. Nieto, A.J. Ramirez-Pastor, Eur. Phys. J. B 43 (2005) 363.
[4] H. Harder, A. Bunde, W. Dieterich, J. Chem. Phys. 85 (1986) 4123.
[5] Z. Gao, Z.R. Yang, Physica A 255 (1998) 242.
[6] H. Holloway, Phys. Rev. B 37 (1988) 874.
[7] Y. Leroyer, E. Pommiers, Phys. Rev. B 50 (1994) 2795.
[8] B. Bonnier, M. Hontebeyrie, Y. Leroyer, C. Meyers, E. Pommiers, Phys. Rev. E 49 (1994) 305.
[9] Y.Y. Tarasevich, V.A. Cherkasova, Eur. Phys. J. B 60 (2007) 97.
[10] V.A. Cherkasova, Y.Y. Tarasevich, N.I. Lebovka, N.V. Vygornitskii, Eur. Phys. J. B 74 (2010) 205.
[11] Y.Y. Tarasevich, N.I. Lebovka, V.V. Laptev, Phys. Rev. E 86 (2012) 061116.
[12] P. Longone, P.M. Centres, A.J. Ramirez-Pastor, Phys. Rev. E 85 (2012) 011108.
[13] D.A. Matoz-Fernandez, D.H. Linares, A.J. Ramirez-Pastor, Eur. Phys. J. B 85 (2012) 296.
[14] I. Lončarević, Z.M. Jakšić, S.B. Vrhovac, Lj. Budinski-Petković, Eur. Phys. J. B 73 (2010) 439.
[15] I. Balberg, N. Binenbaum, Phys. Rev. B 28 (1983) 3799.
[16] T. Natsuki, M. Endo, T. Takahashi, Physica A 352 (2005) 498.
[17] F. Du, J.E. Fischer, K.I. Winey, J. Polym. Sci. B 41 (2003) 3333.
[18] W. Lebrecht, Valdés, E.E. Vogel, F. Nieto, A.J. Ramirez-Pastor, Physica A 392 (2013) 149.
[19] D. Stauffer, A. Aharony, Introduction to Percolation Theory, second ed., Taylor & Francis, London, 1994.
[20] P.J. Reynolds, H.E. Stanley, W. Klein, Phys. Rev. B 21 (1980) 1223.
[21] E.E. Vogel, W. Lebrecht, J.F. Valdés, Physica A 389 (2010) 1512.